MULTISCALE MODELLING OF CREATION AND EVOLUTION OF DEFECTS IN SIC DIODE DETECTORS PLACED AT A NEUTRON FIELD

B. Khorsandi,[1] T.E. Blue,[2] W. Windl[3]

1. Candesco Corporation, Toronto, Ontario, Canada, bkhorsandi@candesco.com
2. The Ohio State University, Columbus, Ohio, USA, blue.1@osu.edu
3. The Ohio State University, Columbus, Ohio, USA, windl.1@osu.edu

ABSTRACT

We discuss a multiscale computer simulation method to study the long-time accumulation of defects for SiC detectors placed in the central reflector of the Gas Turbine-Modular Helium Reactor (GT-MHR) at 500 K. Using Monte Carlo (MC), binary collision approximation (BCA) and kinetic lattice Monte Carlo (KLMC) simulations, we calculate the number of point defects per atom (*PDPA*) for SiC detectors over a 15.7 month reactor refuelling cycle, which is the minimum time when it would be possible to replace the SiC detectors, if that were necessary. We found, for SiC detectors placed at the centre of the GT-MHR's central reflector, the *PDPA* is 1.7×10^{-3} in the depleted region for SiC detectors operated at 500 K for a reactor refuelling cycle, and that approximately half of the defects that are initially created anneal out during that period.

1. INTRODUCTION

Every solid material placed in a neutron radiation field will be degraded due to interactions between neutrons and material atoms. Two major interaction types are neutron scattering and neutron absorption. In the neutron scattering interaction, an energetic neutron transfers some of its energy to the primary knock-on atom (PKA). In the neutron absorption interaction, a neutron will be absorbed by an atom and the resultant atom's subsequent emission of radiation causes the resultant atom to recoil. In both cases, an atom which gains enough kinetic energy will move from its lattice position, and may even hit other atoms in the material, creating more defects. In a long-term exposure, the accumulation of defects degrades the material or electrical properties of the irradiated material. Examples of radiation degradation of material properties are swelling, creep and embrittlement of fuel cladding. An example of radiation degradation of electrical properties of materials would be the changes that would occur in the electrical properties of silicon carbide (SiC) neutron monitors, if they were to be placed in or around a reactor core. These changes would include increased trapping of carriers that are produced in interactions of neutrons (or ions that are generated in a radiator foil) within the detector and decreased carrier mobilities. These changes in SiC electrical properties would modify the pulse height distribution for SiC detectors.

Defects created due to radiation may diffuse and/or evolve in a high-temperature environment. Therefore, if a material can tolerate a high temperature environment, the high temperature may protect it from further degradation. As an example, at room temperature, 4H-SiC detectors rapidly degrade, [1][2] at a rate that is dependent on the neutron flux, but at elevated temperatures the detector performance is stable [3][4].

The study of creation and evolution of defects within a material helps researchers predict at what point (if such a point exists) the material performance becomes stable or how long a material is operationally functional in a nuclear reactor. Based on the best knowledge of authors, there is no a single computer code to be used for these purposes. In this paper, it is explained how several codes, including one written by authors, were used to predict how the defect concentration in a SiC neutron detector would change as a function of neutron fluence and temperature, while placed in a neutron environment, highlighting the central reflector of the GT-MHR. The modelling methodology presented in this paper is useful for other applications, where a solid material is under neutron or ion-particle irradiation.

2. BACKGROUND INFORMATION

2.1 SiC Diode Detector

Per the design of Westinghouse Electric Company, [5] the n-type SiC neutron detector is based on a Schottky diode that detects tritons that are emitted from a LiF radiator layer that is comprised of 90% enriched ^{6}Li. This enriched LiF layer plays an essential role in the functioning of the SiC neutron detector, since tritons create a peak in the detector's pulse height spectra, within the continuum of events that are the result of energy deposition by neutron induced Si and C recoil nuclei. Figure 1 presents the design of a Schottky diode neutron detector. Thermal neutrons may interact with ^{6}Li atoms producing ^{4}He (α) and 2.73-MeV ^{3}H (triton) particles. The tritons pass through an Al layer and deposit a fraction of their energy as ionization in the depleted region of the detector. α particles, which also produce damage in the depleted SiC layer, are shielded by an aluminium layer. Computational analyses made using the TRIM code[1] [6] have shown that an 8-μm aluminium layer between the ^{6}LiF and SiC layers stops all α particles. Stopping α particles from producing radiation damage in the SiC depleted region prolongs the detector lifetime.

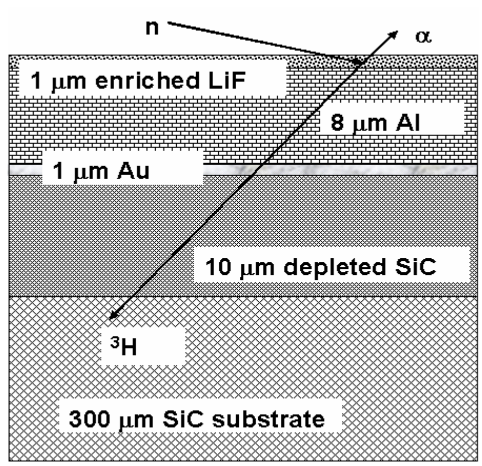

Figure 1: Schottky diode concept. Picture is not drawn to scale. [7]

[1] The TRIM code is part of the SRIM program package.

The SiC detector illustrated in Figure 1 is sensitive to fast neutrons, as well as thermal neutrons. Based upon experimental observations, if the deposited kinetic energy to the struck atom from a fast neutron is more than approximately 200 keV within the detector active volume (the depleted SiC layer), it creates a pulse which exceeds the lower level discriminator (LLD) of the pulse counting system (the level is set to discriminate against gamma ray events) and causes a count.

2.2 GT-MHR

The GT-MHR, a Generation IV nuclear reactor being designed by General Atomics, operates at elevated temperatures. In the GT-MHR design (Figure 2), fuel elements (which are TRISO particles) are surrounded by side and central graphite reflectors. The coolant, helium gas, enters the core at temperatures about 491 °C and exits it at approximately 850 °C [8]. As shown in Figure 3, four radial locations within the graphite central reflector of the GT-MHR were chosen in which to model graphite detector capsules: R153[2] at the outermost ring, R117 in the inwardly adjacent ring, R81 in the next inwardly adjacent ring and R0 at the centre of central reflector. Capsules at R153, R117 and R81 were modelled at six azimuthally symmetric locations. The purpose of capsules was to protect SiC detectors, placed in the capsules, from overheating. [7]

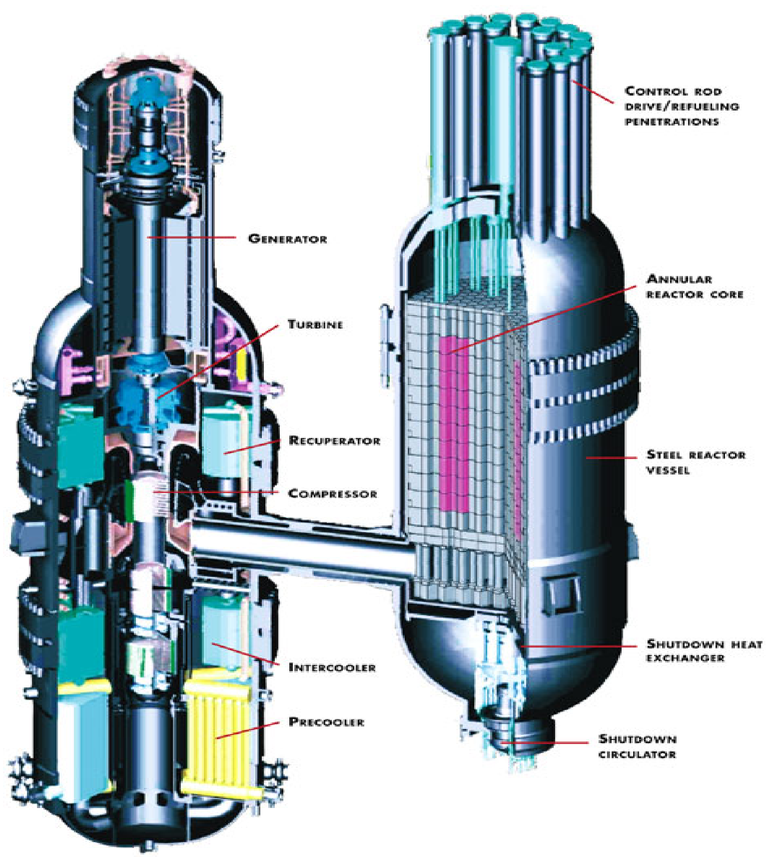

Figure 2: GT-MHR module arrangements. [7]

[2] The number after 'R' is the radial location of the capsule in cm.

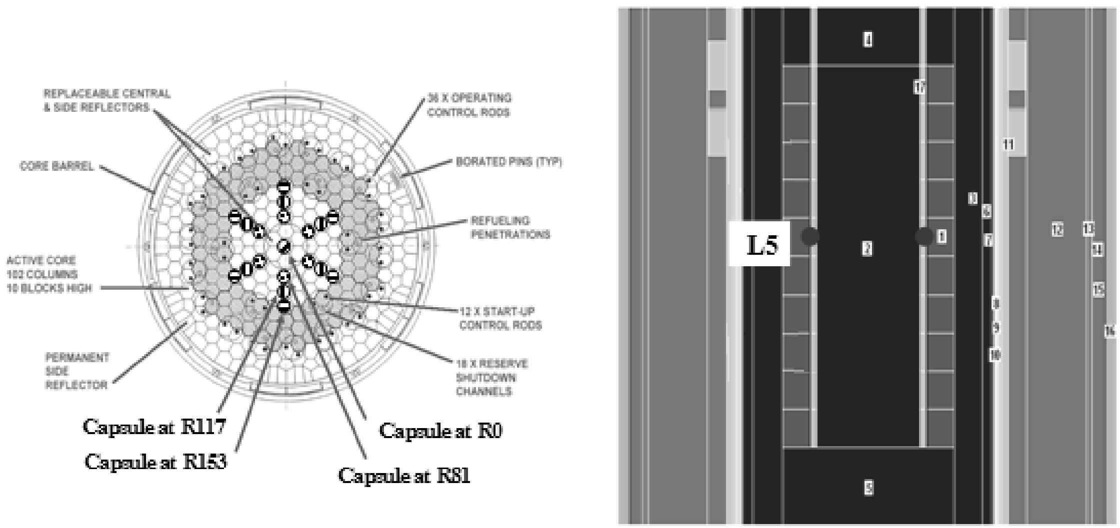

Legend:

1 - Core	5 - Lower Ref.	10 - Gas Duct Shell	14 - Air RCCS
2 - Inner Ref.	6 - Permanent Ref.	11 - Reactor Vessel	15 - Cavity Liner
3 - Outer Ref.	7 - Boron Pins	12 - Reactor Cavity	16 - Concrete
4 - Upper Ref.	8 - Core Barrel	13 - RCCS	17 - Capsule's Tube

Figure 3: Schematics of the GT-MHR. The left figure shows the top view of the GT-MHR. The right figure displays the GT-MHR MCNP5 model. We determined the neutron flux at layer L5. Pictures are not drawn to scale. The capsules are not in the original design and have been added by the authors.

3. MODELLING METHOD

The interaction between neutrons and the detector is more complex than just pulse creation. For example, in order to transfer a kinetic energy of 200 keV (minimum struck atom kinetic energy that leads to the creation of a potentially countable pulse) to an atom through neutron scattering, the minimum required neutron energy is 700 keV for the creation of C recoils and 1.5 MeV for the creation of Si recoils. Neutrons which have energies more than these amounts are rare in a thermal reactor, such as the GT-MHR. On the other hand, neutrons which have energy more than approximately 100 eV are capable of creating defects in the SiC lattice. Defect accumulation degrades the electrical properties and sensitivity of the detector. For the SiC detector, shown in Figure 1, the majority of defects in the SiC depleted region would be created by tritons emitted from the LiF layer, fast neutrons, and 1.3-keV ^{29}Si and 1-keV ^{13}C recoil atoms. The last two particles listed would be created, respectively, via $^{28}Si(n,\gamma)^{29}Si$ and $^{12}C(n,\gamma)^{13}C$ neutron absorption reactions in SiC layers.

In this paper, only point defects are considered. A point defect is a vacancy, interstitial or antisite. A vacancy is an unoccupied site for an atom or ion in a crystal. An atom or ion fitting into the space among lattice atoms would be described as an interstitial atom or ion. An antisite is a defect where, for compounds which have 2 or more atoms, a lattice site is occupied by a wrong atom or ion. For instance, if in SiC, a C lattice site is occupied by a Si atom, then this is called a Si antisite, and if in SiC, a Si lattice site is occupied by a C atom, then this is called a C antisite. In pure SiC, six different point defects may be produced. These are: C interstitial (I_C), Si interstitial (I_{Si}), C vacancy (V_C), Si vacancy (V_{Si}), Si antisite (Si_C), and C antisite (C_{Si}).

Whereas higher neutron flux and neutron fluence lead to the accumulation of a greater number of defects, operation at a reasonably high temperature[3] helps the detector to tolerate the reactor environment for a longer time. This is because some defects may recombine and vanish. For example, a V_C may recombine with an I_C and create a C atom in its original site (such as $V_C + I_C \rightarrow$ C in its original site), which is not a defect anymore. Modelling the creation and evolution of defects is an important step in estimating the functional life of SiC detectors inside of the nuclear reactor.

In this paper, we calculate the number of point defects per atom (*PDPA*) for SiC detectors after a reactor refuelling cycle. There is no single code available to determine all the information given in this paper, including:

- The neutron flux and energy spectrum at the studied locations in the GT-MHR;
- Neutron reaction rates with ^{6}Li, Si and C atoms of the SiC detector;
- The number of defects created by energetic neutrons, tritons, Si and C atoms in the depleted region of SiC; and
- The annealing effect (reactions between defects).

Therefore, the authors used a combination of several codes, as follows.

Neutron Flux and Neutron Energy Estimation

Monte Carlo N-Particle, version 5, (MCNP5) [9] was used to estimate the neutron flux and neutron energy spectra within the capsules where the SiC detectors would be placed. In our MCNP5 model of the GT-MHR, the central reflector consists of graphite hexagonal elements. The active core consists of an assembly of hexagonal graphite fuel elements (blocks) containing blind holes for fuel compacts and full-length channels for helium coolant flow. The fuelled region of the core was represented in the MCNP5 model as a homogenous mixture of uranium, oxygen, silicon, boron and carbon. Also, six prismatic elements of the outer replaceable reflector were inserted into the hexagon defining the active core, in order to model the real geometry, as closely as possible. A more detailed description regarding our MCNP5 modelling of the GT-MHR can be found in Refs [10] and [11].

Neutron Reaction Rate Estimation

MCNP5 was used to calculate the reaction rates for ^{6}Li(n,α)^{3}He reactions in the LiF layer and neutron absorption and scattering reactions with Si and C atoms in the depleted SiC, for the determined neutron energy spectrum. In this MCNP5 model, the SiC detector was modelled as being at the centre of a sphere. A source of neutrons was defined at the surface of the sphere, with a neutron energy spectrum corresponding to the neutron flux that was calculated in step one, as described immediately above. The neutron source was emitted from the spherical surface with a directional bias, which created a higher track density toward the centre of the sphere, where our detector was placed. The radius of the sphere was 0.1 cm.

[3] At too high temperatures, electrons are promoted across the SiC semiconductor band gap by thermal excitation. Also, the detector contacts and cables would be damaged.

For neutron absorption reactions in Li, Si and C, the F4:N tally and FM cards were used to determine the number of $^{6}Li(n,\alpha)^{3}He$ reactions in the LiF layer and the number of $^{28}Si(n,\gamma)^{29}Si$ and $^{12}C(n,\gamma)^{13}C$ reactions in the depleted SiC, for the SiC diode detector illustrated in Figure 1.

The MCNP5 model for neutron scattering reactions was similar to the model described in above, but the PTRAC card in MCNP5 was used to determine the probability that a neutron, which enters the SiC volume, will interact with a Si or C atom therein. The PTRAC output file gave the neutron characteristics (energy, position and direction cosines), before and after each collision, as well as the type of PKA that is created in a collision. Based on conservation of momentum, the PKA characteristics (atomic species, energy, position and direction cosines) were determined. [7]

Estimation of Number of Defects Created

The above information was used to determine the number of defects using TRIM. TRIM, a Monte Carlo code developed by Ziegler, was used to determine the number of defects created by the stated projectiles (tritons, ^{29}Si and ^{13}C recoils, and scattered PKAs) in the SiC depleted region. TRIM is a binary collision approximation (BCA) code that determines the collision characteristics between projectiles (ions or atoms) and the target atoms. The inputs for TRIM are types, energies, positions and directions of incident projectiles, and densities, thicknesses, displacement energies (E_d) and binding energies of target atoms. The E_d values were set equal to 20 eV and 35 eV for C and Si, respectively, to be consistent with Gao et al [12]. The other information was either determined in the above stages of the calculation or default values in TRIM were used.

Spatial Distribution of Defects

The TRIM code gives only the spatial distribution of vacancies, not interstitials. Also, TRIM models the target materials as amorphous, not as crystalline. To overcome these issues, MARLOWE [13] was used in conjunction with TRIM. MARLOWE is a program for simulating atomic collision processes in crystalline solids based on the BCA. In MARLOWE, the target can be modelled as a crystal. Also, MARLOWE gives the positions of vacancies and interstitials, within some uncertainties. However, MARLOWE is difficult to use. Therefore, we used TRIM to adjust two of MARLOWE's input parameters (EBND[4] and EQUIT[5]) for each projectile energy that was analyzed, until the MARLOWE output for the number of C and Si-vacancies matched the TRIM output for these quantities. The spatial distributions of defects were used as an input for the KLMC code.

Defects Evolution

The TRIM and MARLOWE codes assume that the target is at zero temperature (there is no annealing effect). In order to predict the impact of temperature and model the annealing process, we developed a KLMC code that we named MCASIC. In the KLMC, defects hop randomly based on their diffusion coefficients, which are functions of ambient temperature. For each hop, MCASIC estimates the real time and advances the

[4] EBND is the energy parameters of the binding model.
[5] EQUIT is the minimum kinetic energy for an atom to continue in motion.

clock. If the distance between two defects becomes less than the capture radius for this defect pair (another KLMC code was written to determine the capture radius for different defect pairs in SiC), several different processes may occur depending on the nature of defects. They may recombine and eliminate each other, or they may recombine and create one defect instead of two (such as $V_C + I_{Si} \rightarrow Si_C$). Sometimes if two defects (such as I_C-I_C) become close enough, they may significantly influence their diffusion properties. In this case, a defect cluster is created. Usually, defect clusters have less mobility than point defects. For further information about KLMC, we refer the reader to more specific papers, such as [14][15].

Usually, traditional KLMC codes simulate the damage annealing from 1×10^{-3} s up to 100 s. In this paper, 10 s of the annealing process for triton and ^{29}Si recoils at 500 K is modelled. It should be noted that in this paper, only the defects evolution for a detector placed at R0, where there is no damage due to fast neutrons, is presented. The number of defects created by ^{13}C recoils is not included since the absorption cross section for ^{12}C is very small and, therefore, the number of defects created by ^{13}C recoils would be negligible (the number of ^{29}Si recoils is approximately 50 times more than the number of ^{13}C recoils).

4. RESULTS

Figure 4 shows the differential neutron flux vs. energy for locations R153, R117, R81 and R0 in the capsule. The total neutron fluxes for R153, R117, R81 and R0 are $2.1\text{x}10^{11}$, $4.3\text{x}10^{11}$, $5.2\text{x}10^{12}$ and $4.4\text{x}10^{13}$ n/cm^2, respectively. Although, there is a lack of good statistics, particularly at R81, it is seen that the fast neutron flux declines dramatically by decreasing the radial location of the capsule in the GT-MHR central reflector. The Maxwellian thermal neutron spectrum can clearly be identified in the spectra for R117, R81 and R0.

Figure 5 shows the number of defects created by specified projectiles. As can be seen, neutrons at R0 cannot create defect via scattering, since the energy of neutrons in that region is less than the E_ds for Si and C. On the contrary, neutrons at R153 transfer enough kinetic energy to SiC atoms to create a number of defects.

A ^{29}Si recoil creates, on average, more defects than a ^{13}C recoil and the tritons. The reasons are: 1) tritons lose part of their energy while passing through LiF, Al and Au layers; 2) tritons lose a major part of their energy due to electronic stopping that does not create damage; 3) the masses of SiC atoms are closer to the mass of ^{29}Si recoils than the mass of a triton, therefore, the kinetic energy transferred to the struck atom from a ^{29}Si is more than that from a triton, if both have similar energy; 4) ^{29}Si energy is more than ^{13}C energy; and 5) E_d for Si is more than E_d for C. The rationale for the last statement is simply that if a ^{13}C recoil hits a Si atom in the lattice, the transferred kinetic energy may not be enough to create any defect. For a ^{29}Si recoil which hits a C atom in the lattice, the probability of not transferring enough energy to create a defect is lower.

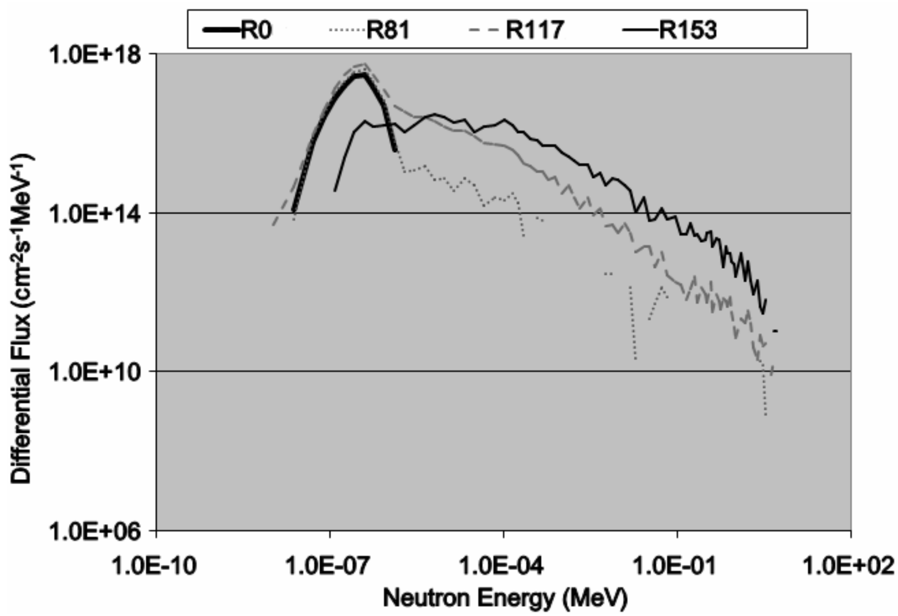

Figure 4: Differential neutron flux vs. energy for R153, R117, R81 and R0 (P = 600MW$_{th}$). [7]

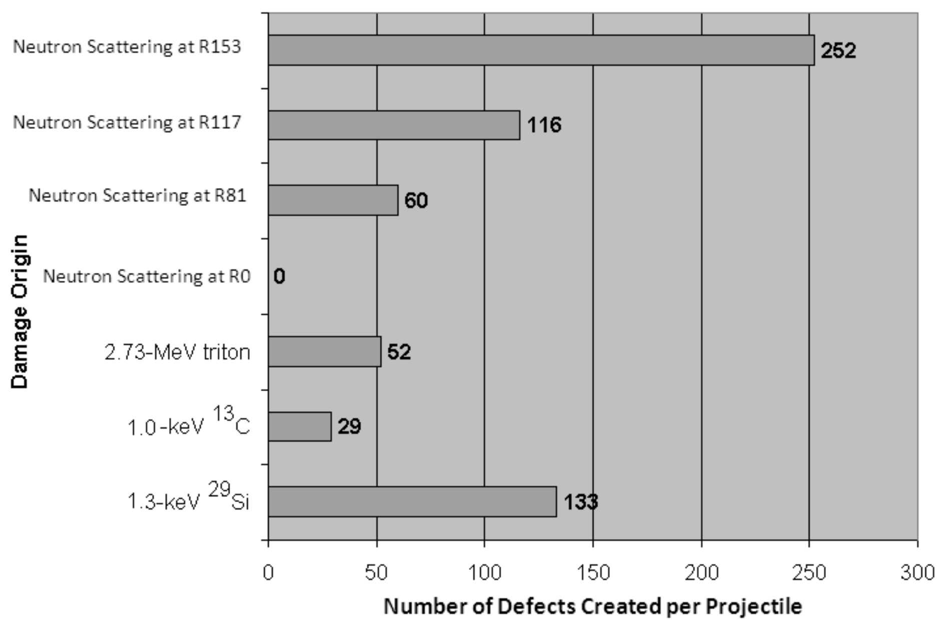

Figure 5: Average number of defects created per neutron absorbed or scattered. It should be noted that 39% of the tritons that are born in the LiF reach the SiC depleted region (the geometric efficiency), for the SiC detector geometry shown in Figure 1.

Figure 6 shows the *PDPA* for the depleted SiC region after one reactor refuelling cycle, which is approximately 15.7 months, assuming there is no annealing. As can be seen the number of defects created at R153 is more than the numbers of defects created in SiC at other radial locations, by more than one order of magnitude. The value of 1.6 for

PDPA after one reactor refuelling cycle means that on average each atom in the SiC depleted region has been displaced 0.8 times. With this defect density, if annealing were not to occur, then the SiC would become an amorphous material and lose its semiconductor properties.

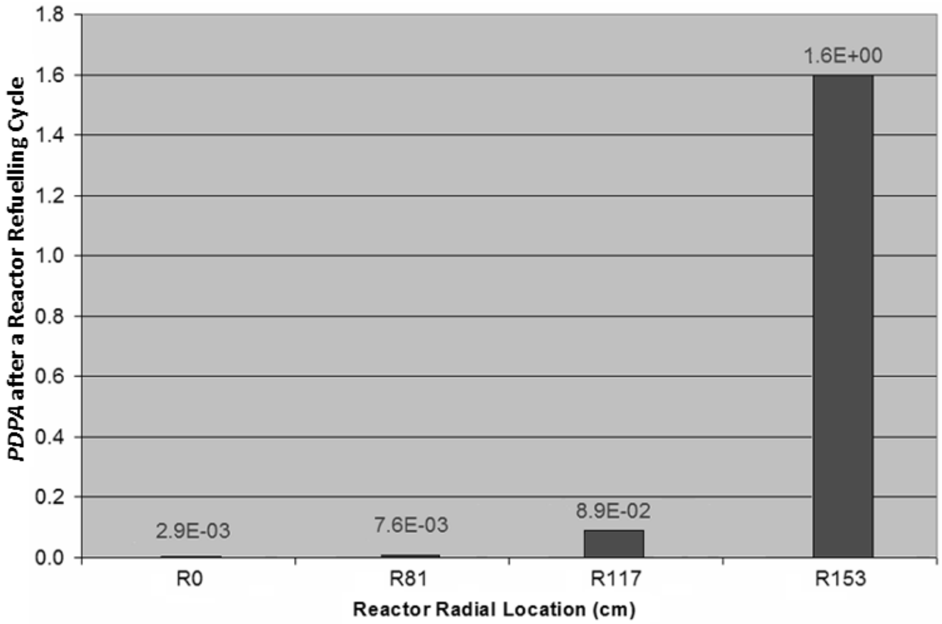

Figure 6: *PDPA* for the depleted region of a SiC detector after one reactor refuelling cycle (15.7 months) for different radiation locations in the central reflector of the GT-MHR.

Since the GT-MHR is a high temperature reactor, there is a high probability that most defects created would vanish within some short time after their creation, when defects interact with each other. Figure 7 shows the capture radii as functions of temperature, for temperatures from 200 K to 1000 K, for defect pairs in 4H-SiC. The capture radii for defect pairs decrease with increasing temperature, in agreement with the findings of [14]. Considering some computational fluctuations, the largest capture radius in the studied temperature range belongs to I_{Si}-V_{Si}. These two defects can capture each other at a distance of 1.46 nm when the temperature is 500 K. The smallest capture radii belong to Si_C-V_{Si} and V_{Si}-V_{Si}, respectively. At 500 K, those defect pairs may not interact with each other until their distances fall below 0.48 nm and 0.5 nm, respectively. We found that there is no appreciable interaction between C_{Si} and I_C defects. It should be noted that although the capture radius for a defect pair decreases with increasing temperature, since defects move faster at a high temperature, there is a greater probability for defect interaction.

For a SiC detector placed at the GT-MHR R0, the MCNP5 modelling shows that 1.7×10^{13} 2.73-MeV tritons are born in the LiF[6] during one GT-MHR refuelling cycle. Figure 8 displays the fraction of defects remaining after annealing at 500 K for 10-sec annealing for different tritons energies (triton energy while entering the SiC). As can be seen in Figure 8, the effectiveness of the annealing process decreases with increases in

[6]The ^{6}Li burn-up has been neglected.

the triton energy. For example, if a 50-keV triton hits the SiC target, after a 10-sec annealing time, approximately 70% of the defects created by it will have vanished. However, if a 2050-keV triton hits the target, only approximately 30% of the defects would have vanished after a 10-sec annealing time. This is because the defects of the cascade have a larger spatial separation at higher energies and cannot reach each other to recombine.

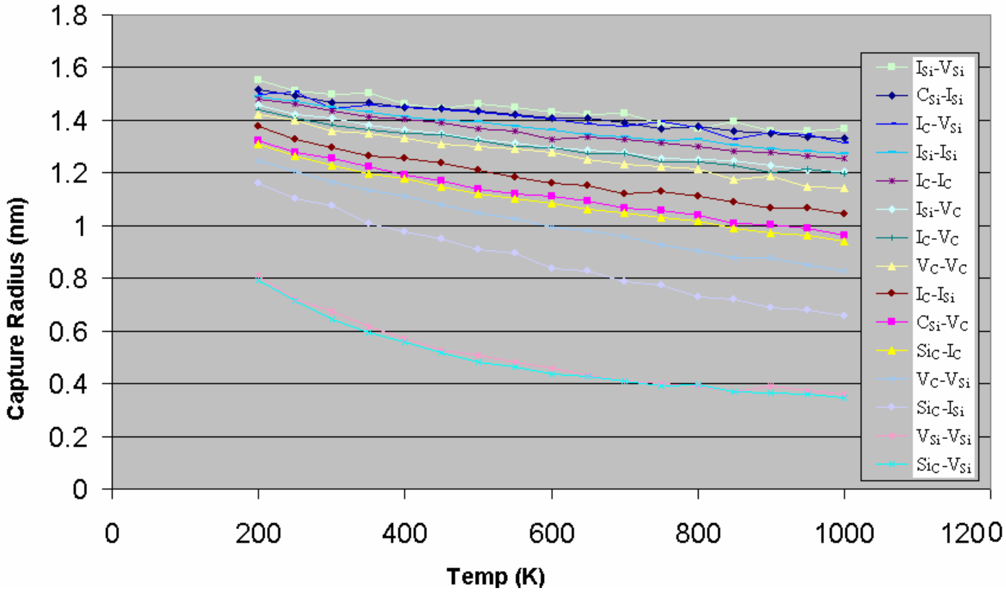

Figure 7: Capture radii for defect pairs in 4H-SiC at different temperatures

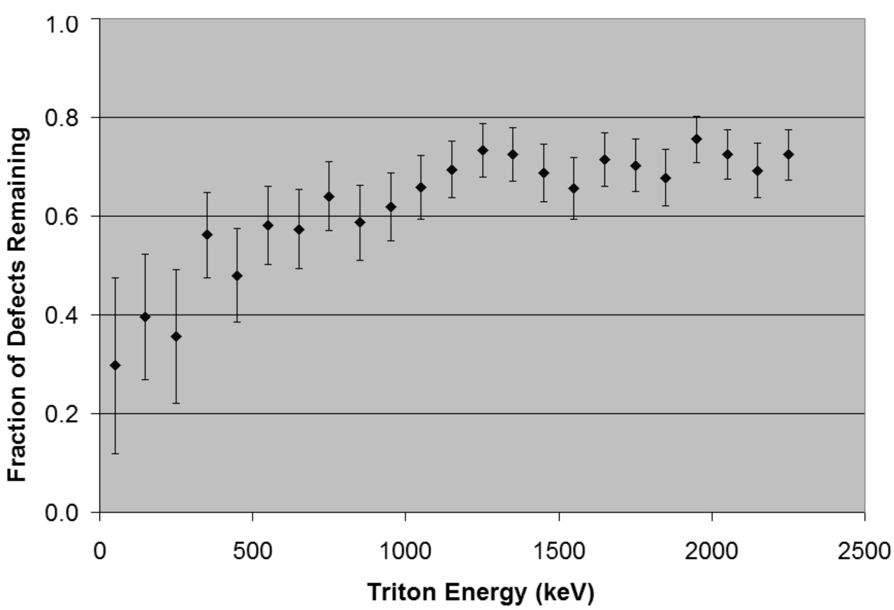

Figure 8: Fraction of defects remaining after 10-sec annealing to the number of defects before annealing. The uncertainties were calculated based upon the number of defects that remained, assuming binomial statistics.

Also, MCNP5 modelling shows that $8.1x10^{11}$ ^{29}Si recoils are born in the SiC, during one GT-MHR refueling cycle. Initially, the average number of defects created is 133 per ^{29}Si recoil. The MARLOWE+KLMC results show that the number of defects created by a ^{29}Si recoil reduces to 9 after 10-sec annealing at 500 K. In other words, approximately 90% of the defects created by ^{29}Si recoils disappear in the first 10 seconds of annealing.

Our modelling shows that *PDPA* for the depleted region of a SiC detector placed at GT-MHR R0 is approximately $1.7x10^{-3}$ after 15.7 months of operation at 500 K, if only the first 10-sec annealing after defect cluster creation is considered. Without the annealing effect, *PDPA* would have been $2.9x10^{-3}$. Therefore, the annealing process (via defect recombination) decreases the amount of defects by a factor of about 1.7. Assuming that the effect of the defects are the same, the decrease in the number of defects by factor of 1.7 means that the detector can tolerate the environment for a time which is longer by a factor of 1.7, compared to the case where annealing is neglected.

5. CONCLUSION

Using a multiscale modelling methodology, we have developed a simulation method to estimate the number of defects for SiC detectors placed in the central reflector of the GT-MHR. Also, considering only 10 s of annealing, we studied the evolution of defects created in the detectors placed at GT-MHR R0 at 500 K. We found that at 500 K, the *PDPA* is $1.7x10^{-3}$ in the depleted region for SiC detectors placed at GT-MHR R0 for a refuelling cycle, and that approximately half of the defects that are initially created anneal out during that period.

In the calculations, only the first 10-sec after damage creation was considered. From these results, we currently cannot predict the changes in functionality of the detector, because we do not know the relationship between *PDPA* and changes in detector performance. A final step in our modelling process will be to evaluate the influence of the defects on the carrier mobility and other electrical properties of SiC, and to predict how these changes in the electrical properties of SiC affect the count rate of the power monitor. Identification and modelling of the critical *PDPA* for detector failure is the subject of our ongoing research.

The authors believe that the modelling methodology described in this paper, with some modifications, can be used to estimate the number of defects in other reactor materials and to study the effect of temperature.

ACKNOWLEDGEMENTS

This material is based upon work supported by the US Department of Energy under the NERI program Award No. DE-FG-07-02SF22620 and NERI Project Number 02-207. Any opinions, findings, and conclusions or recommendations expressed in this material are those of the authors and do not necessarily reflect the views of the Department of Energy.

We thank Dr. Don Miller, Dr. Mehdi Reisi Fard, Jonathan Kulisek, and Vijiayalakshm Krishnan for very helpful discussions.

REFERENCES

[1] M. Reisi Fard et al., “Evaluation of the SiC Semiconductor Diode Detector Degradation in a Fast Neutron Flux”, 5th International Topical Meeting on Nuclear Plant Instrumentation, Control and Human-Machine Interface Technologies (NPIC & HMIT 2006), Albuquerque, NM, Nov 12-16 (2006).

[2] L. Scheick et al., “Displacement Damage-Induced Catastrophic Second Breakdown in Silicon Carbide Schottky Power Diodes,” IEEE Transactions on Nuclear Science, 51, 6 (2004) 3193-3200.

[3] F.H. Ruddy et al., “Power Monitoring in Space Nuclear Reactors Using Silicon Carbide Radiation Detectors,” Proceeding of the Space Nuclear Conference, San Diego, California, Jun 5-9 (2005).

[4] S. Sciortino et al., “Effect of Heavy Proton and Neutron Irradiations on Epitaxial 4H-SiC Schottky Diodes,” Nuclear Instruments and Methods in Physics Research A, 552, 1-2, 21 (2005) 138-145.

[5] A. R. Dulloo et al., “The Neutron Response of Miniature Silicon Carbide Semiconductor Detectors,” Nuclear Instruments and Methods in Physical Research Section, A, 422 (1999) 47-48.

[6] F.J. Ziegler, “SRIM-2003,” Nuclear Instruments and Methods in Physics Research, B, 219-220 (2004) 1027-1036.

[7] B. Khorsandi et al., “Monte Carlo Modeling of Count Rates and Defects in a Silicon Carbide Detector Neutron Monitor System, Highlighting GT-MHR,” Nuclear Technology, 159, 2, Aug (2007) 208-220, Copyright August 2007 by the American Nuclear Society, La Grange Park, Illinois.

[8] M.P. Labar et al., “Status of the GT-MHR for Electricity Production,” World Nuclear Association Annual Symposium, London, Britain, 3-5, Sep (2003); and M. P. Labar, “The Gas Turbine—Modular Helium Reactor: A Promising Option for Near Term Deployment,” GA-A23952, General Atomics, Apr (2002).

[9] R. A. Forster et al., “MCNP Version 5,” Nuclear Instruments and Methods in Physical Research Section, B, 213 (2004) 82-86.

[10] B. Lohan, “Nuclear Reactor Power Monitoring Using Silicon Carbide Semiconductor Radiation Detector in Gas Turbine Modular Helium Reactor,” Master Thesis, The Ohio State University (2004).

[11] T.E. Blue et al., “Neutron Damage in SiC Semiconductor Radiation Detectors in the GT-MHR,” JAI, 3, 8 (2006), Reprinted, with permission, from the Journal of ASTM International, Vol. 3, Issue 8, copyright ASTM International, 100 Barr Harbor Drive, West Conshohocken, PA 19428.

[12] F. Gao et al. “Defect Production, Multiple Ion-Solid Interactions and Amorphization in SiC,” Nuclear Instruments and Methods in Physics Research, B, 191 (2002) 487-496.

[13] M.T. Robinson, “MARLOWE Binary Collision Cascade Simulation Program, Version 15a, a Guide for Users,” Sep 1 (2001).

[14] K.M. Beardmore et al., “Diffusion Mechanisms and Capture Radii in Silicon,” Nanotech, 1, 9 (2002).

[15] M.J. Caturla et al., “Comparative Study of Radiation Damage Accumulation in Cu and Fe,” Journal of Nuclear Materials, 276 (2000) 13-21.